Lawrence Berkeley National Laboratory
Recent Work

Title
A TEM STUDY OF RHODIUM ON GaAs: REACTIONS AND MORPHOLOGY

Permalink
https://escholarship.org/uc/item/2dk945f6

Author
Packer, S.

Publication Date
1987-05-01

eScholarship.org Powered by the California Digital Library
University of California

LBL-23536 c.2

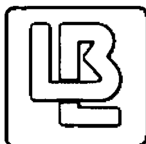

Lawrence Berkeley Laboratory

UNIVERSITY OF CALIFORNIA

Materials & Chemical Sciences Division

RECEIVED
LAWRENCE
BERKELEY LABORATORY

JUL 1 4 1987

LIBRARY AND
DOCUMENTS SECTION

National Center for Electron Micrsocopy

A TEM STUDY OF RHODIUM ON GaAs: REACTIONS AND MORPHOLOGY

S. Packer
(M.S. Thesis)

May 1987

TWO-WEEK LOAN COPY
This is a Library Circulating Copy
which may be borrowed for two weeks.

Prepared for the U.S. Department of Energy under Contract DE-AC03-76SF00098

LBL-23536 c.2

DISCLAIMER

This document was prepared as an account of work sponsored by the United States Government. While this document is believed to contain correct information, neither the United States Government nor any agency thereof, nor the Regents of the University of California, nor any of their employees, makes any warranty, express or implied, or assumes any legal responsibility for the accuracy, completeness, or usefulness of any information, apparatus, product, or process disclosed, or represents that its use would not infringe privately owned rights. Reference herein to any specific commercial product, process, or service by its trade name, trademark, manufacturer, or otherwise, does not necessarily constitute or imply its endorsement, recommendation, or favoring by the United States Government or any agency thereof, or the Regents of the University of California. The views and opinions of authors expressed herein do not necessarily state or reflect those of the United States Government or any agency thereof or the Regents of the University of California.

LBL-23536

A TEM STUDY
OF
RHODIUM ON GaAs:
REACTIONS AND MORPHOLOGY

Stacy Packer

Master's Report

May 1987

Department of Materials Science and Mineral Engineering
University of California, Berkeley
and
Materials and Chemical Sciences Division
Lawrence Berkeley Laboratory
University of California
Berkeley, California 94720

A TEM Study of Rhodium on GaAs: Reactions and Morphology

Stacy Packer

Abstract

The interfacial reaction between rhodium films and n-type GaAs in the temperature range of 300° to 700°C has been examined using TEM and electron diffraction methods. The reaction between Rh and GaAs produces a layered structure of Rh/RhGa/$RhAs_2$/GaAs based on RBS and TEM. Above 300°C, the RhGa phase has an orientation relationship of [011]RhGa // [100]GaAs. In cross-section, an interpenetrated layered structure was observed with equiaxed RhGa above columnar grains of RhAs2. Rhodium is the moving species as suggested by Kirkendall voiding observed at the RhGa interface. The activation energy of the reaction was calculated to be 1.35 eV. The interface between the reacted layer and GaAs was smooth at 450° and 20 minutes of annealing but showed 10 nm periodic penetrations when annealed at 400° for 90 minutes. Interface roughness may influence the low barrier height reported for the Rh Schottky diode annealed at 400°.

Table of Contents

Abstract..1

Introduction...2

Experimental 3

Results

A. Planview Studies 4
300° 20 Minutes
400° 20 Minutes
500° 20 Minutes
700° 20 Minutes

B. Cross-sectional Studies 7
350° 20 Minutes
400° 90 Minutes
450° 20 Minutes

Discussion of Results 9

Conclusions...13

Acknowledgements 14

References...15

Figure Captions 16

Tables 18

Figures 22

Introduction

Stable, reproducible metal contacts with good ohmic or rectifying electrical properties are important for making advanced III-V compound devices such as high mobility heterojunction transistors, HEMTs. The science and technology of metal contacts to GaAs is a complex problem. The deposited metal reacts with the compound semiconductor forming phases that include (at least) 3 elements; binary phases can form with both group III and group V elements, or ternary phases are produced. The reacted contacts have poor mechanical properties and can be non-uniform spatially. The properties of a single metal are rarely sufficient to make a good contact with respect to electrical, spatial and mechanical properties, so contacts are usually made with multiple layers of deposited metals. Often the processing window is so narrow that only a specific recipe of cleaning and process temperature produces the desired contact.

The solid phase reactions and the effect of metallurgy on electrical properties must be understood to improve the performance of electrical contacts. To do this the reactions and morphology of single layers of metal annealed on compound semiconductor must be studied. Reports on interfacial reactions for M/GaAs contacts have concentrated on only a few metals, such as Au, Pt, and W,(1-6) unlike the case for silicon contacts where there has been extensive investigation. Recently, the metallurgy of the M/GaAs interfaces of near noble and refractory metals have attracted attention (7-12), due to advancements in compound semiconductor technology requiring new processing techniques for GaAs devices. Rutherford backscattering spectroscopy (RBS) and transmission electron microscopy (TEM) are the most revealing team of complementary techniques for studying thin film reactions on semiconductors. Information on chemical composition as a function of depth is found from RBS and HIRBS (heavy ions give better mass resolution for light elements such as gallium and arsenic

(13)). Electron microscopy can supply information on the structure of the reacted phases, their orientation relationship with the semiconductor substrate and the morphology of the film and the interface between film and substrate. Further complementary techniques include x-ray diffraction and I-V dependence.

Many other contact systems may possibly work well but have not yet been carefully studied; one system which may be promising is the Rh-GaAs Schottky contact. Work by K.M. Yu (12) shows good diode behavior with rhodium on GaAs when annealed at 350°C and from 450 and 500°, (figure 1) but between these temperatures the behavior of the contact is poor, as reflected by the decrease in barrier height. The purpose of this study is to characterize the Rh/GaAs reacted interface using the transmission electron microscope. A spatially resolved picture of the metal/GaAs interface, along with RBS and barrier height information will provide further information on how the contact is affected by temperature.

Experimental

Rhodium was deposited on semi-insulating n-type (100) GaAs substrates by electron beam evaporation. Before deposition, the wafers were etched in 50% HCl solution for 1 minute, rinsed, and blown dry with N_2. Rhodium was deposited to a thickness of 12 nm or 80 nm at a base pressure of 10^{-6} Torr. The metallized wafers were cut into ~ 1 cm^2 pieces and capped on all sides with about 150 nm of SiO_2 film, deposited by plasma-enhanced chemical vapor deposition at a temperature of 150 °C. The 12 nm Rh/GaAs samples were annealed at 300°, 400°, 500°, 700°C for 20 minutes and the 60 nm samples were annealed at 350° for 20 minutes, 400° for 90 minutes and at 450° for 20 minutes.

The 12 nm thick layers were used to examine large ares of the reacted layer in planview after removing the GaAs substrate while the 80 nm samples were made into cross-sections to see the interface between the reacted layer and the substrate. Cross-section samples were

cleaved along <100> and metallized faces glued together with epoxy. Two spacer pieces of scrap GaAs were used to "beef-up" dimensions to fill the entire slot in the 3 mm TEM specimen grid. A lapping tool was used to flatten one face of the sandwich, then the sample was turned over and thinned to 2 mils on 600 grit polishing wheel, then polished down to .3 um alumina. Ion milling using a liquid N_2 cold stage with conditions of 12° tilt, 5 KeV 0.5 mA Ar+ beam current to make the samples electron transparent. Planview samples were cleaved, mounted metal side down on polishing disks, and thinned to a thickness of 2 mils on 600 grit polishing paper, then completed by chemical thinning with MeOH saturated with chlorine gas. A gravity fed jet was used to impinge the MeOH solution onto the GaAs backside of the Rh/GaAs interface thereby removing the GaAs. The chemical etching was complete when a red transparent region was observed at 50X.

Results

A. Planview Transmission Electron Diffraction and Microscopy

Planview samples made from GaAs deposited with 12 nm of Rh were annealed at 300, 400, 500, and 700°C each for 20 minutes then examined on the Phillips 301 TEM.

300°C 20 Minute Anneal

A diffraction pattern with the electron beam normal to the (100) plane of GaAs from the 300° annealed Rh/GaAs sample is shown in figure 2a. Figure 2b is the bright field image showing a grain size of about 6.5 nm. The diffraction pattern consists of continuous polycrystalline rhodium rings and a reaction product whose spacings all fit those of $RhAs_2$. Rhodium is an fcc structure with a_0=.380nm. Its presence is confirmed by the high intensity of the {111} ring. This pattern and that of [100]GaAs was used as an internal calibration for the other lattice spacings measured. Table 1 gives the spacings of $RhAs_2$, RhAs, RhGa, and

Rh and the interplanar distances calculated from measured distances. $RhAs_2$ is monoclinic with a=0.604, b=0.608, c=0.613 nm and β= 114.33°. RhAs is orthorhombic (b31, MnP) where a=0.565, b=0.358, c=0.600 nm. RhGa is a cubic CsCl type structure with a_o=0.301 nm. The strong texture of the pattern is from the polycrystalline reaction product in thin film form. All the distances measured can be identified as $RhAs_2$.

No unique spacings or orientations are seen for RhGa or RhAs at this temperature. Note the lattice parameters of RhAs and RhGa are all included in those of $RhAs_2$. The lowest order, central reflections do not have sufficient accuracy to conclusively identify $RhAs_2$. The angle between the (002) and $(11\bar{2})$ planes were calculated and measured to be 51° and (200) and $(21\bar{1})$ to be 39° in the $RhAs_2$ system. There could also be reflections from the RhAs system where a 52° angle is calculated between $(11\bar{1})$ and $(10\bar{2})$ planes. To further complicate matters, RhGa (100) and (011) are at 90° angles as are (020) and (102) $RhAs_2$, which all share the same spacings.

From the measured diffraction pattern, it can only be said that either $RhAs_2$, RhAs, or both are present at 300°; they are not uniquely definable. The problem with identifying what MAs phase is present stems from the low symmetry and high similarity of the monoclinic $RhAs_2$ and orthorhombic RhAs. CBED would be a possible method to determine crystal symmetry if the grain size was increased.

The reflections show strong texture of the fine grained film. This suggests an energetically favorable crystallographic arrangement of the reaction product on the GaAs substrate at this temperature. Figure 2c is a schematic of the orientation of the strongest reflections of reaction product, showing four-fold texturing. The arcs in the figure mark planar spacings measured.

400 ° 20 Minutes

Annealing at 400 ° for 20 minutes leaves no unreacted Rh on the thin film planview specimens (figure 3). The texturing of the reacted phases is less, in fact the 0.215 nm spacing can be called a textured ring indicating less restriction on possible orientation of the reacting phases. The grain size of the phases has increased to ≈12 nm (figure 3b). Again, the spacings measured correspond with $RhAs_2$ (table 2). However, the $(11\bar{1})$ spacing of $RhAs_2$ unambiguously identifies its presence since 0.393 nm is significantly different than spacings of RhAs. Similar to the 300 ° case, the presence of RhAs cannot be confirmed or denied. The angle between the 0.27 nm reflections are the same as at 300 °.

500 ° 20 Minutes

After 20 minutes at 500 ° the diffraction pattern shows less texture compared to those at lower temperature (figure 4). The grain size has increased to 29 nm. The weakening of texture may indicate removal of orientation requirements for low energy configurations. The $(11\bar{1})$ spacing of $RhAs_2$ is now present in the diffraction pattern oriented to the [100]GaAs pole. Table 3 shows the same spacings as at low temperature with the addition of faint, hexagonally arranged reflections with spacing of 0.517 nm which corresponds to $(10\bar{1})RhAs_2$.

700 ° 20 Minutes

The 700 ° anneal shows the completion of the $RhAs_2$ rings; only a small amount of texture remains. The grain size of the reaction product has increased to 54 nm, some grains possibly exhibit twinning (figure 5). Table 4 shows the same spacings seen before, but with the entire range of $RhAs_2$ between 0.279 and 0.254 nm all present on one diffraction pattern oriented to the [100]GaAs pole. The intensity of the reflections on perpendicular axes are due to the RhGa phase (CsCl) which can be discerned with the $RhAs_2$ pattern. The (100)

and (011) reflections form the perpendicular arrangement seen in the diffraction pattern. There are two 90° orientations of the RhGa, as presented in figure 6:

<011>RhGa // <022>GaAs

<011>RhGa // <0$\bar{2}$2>GaAs

[0$\bar{1}$1]RhGa // [100]GaAs.

B. Cross-Sectional Electron Microscopy and Diffraction

Cross-section samples were made with 60 nm thick Rh on GaAs annealed at 350° for 20 minutes, 400° for 90 minutes, and 450° for 20 minutes. Specimens were examined on the Siemans 102 transmission electron microscope.

350°, 20 Minute Anneal

Figure 7a is a cross-sectional image of the 350° annealed sample oriented to the [100]GaAs pole. The reacted layer can be seen in this image, the thickness is 22 nm. There are two bright regions of missing material above and below the reacted region. These could be voids or an artifact of ion milling. From a collection of micrographs at this temperature, it appears that this interface is fairly smooth. The etch rate of the Rh is much lower than that of Ga and As because of how much heavier atomic Rh is compared to GaAs making it difficult to make good samples yielding a clear interface. The selected area diffraction pattern shows [110] GaAs, unreacted Rh rings and reflections from the reacted layer; as for the planview DP's, everything fits $RhAs_2$.

400° 90 Minute Anneal

After annealing at 400° for 90 minutes the reacted layer has thickened to ~ 96 nm (figure 8). Two micrographs are needed to show the features of the reacted layer and inter-

face. Figure 8a is from a thin region of the specimen where the grain structure showing 2 layers is visible. The layers are distinguished as two types of grains in the reacted structure where the grains near the GaAs interface are columnar 10nm wide and 40 nm high, indicating a prefered growth direction. On top of these, the grains are equiaxed and 10 nm wide. Above and below the equiaxed grains a thin white band of possible native oxide layer can be distinguished. The presence of a native oxide layer when metal is deposited on chemically cleaned GaAs or silicon is well established. On top of this structure is about 55 nm of voided unreacted rhodium. Figure 8b shows a thicker region of the specimen where the reacted layer/substrate interface is intact showing roughness on the order of 10 nm due to penetration of the reacted layer into the GaAs. Figure 8c is a schematic.

Lattice images were used to calculate spacings for phase identification. The columnar grains had a measured spacing of 0.27 nm, corresponding to (211)$RhAs_2$. These lattice planes were normal to the [110] GaAs pole indicating preferred orientation, as was observed for the thin 12 nm films.

450° 20 Minutes

The reacted layer in the sample annealed at 450° for 20 minutes has the same layered structure as at 400° specimen. The layer is now 130 nm thick and shows separation into two grain structures with a ratio of about 1:4. It should be noted that the boundary between structures is interpenetrated, and the interface between the reacted layer and GaAs is smooth, unlike the 400° specimen. At this temperature the grains are coarser than at 400°. The columnar grains are 15 nm wide and 60 nm high and the equiaxed ones are 40 nm in diameter, based on measurement from the micrographs. Not all the grains in the lower structure are columnar; even at the interface some may be equiaxed.

Lattice fringe images of the top-most voided layer confirms the presence of unreacted rhodium. Below this, the equiaxed grains were measured to have a spacing of 0.301 nm, corresponding to (100)GaAs. For the columnar grains, spacings of 0.276 and 0.267 nm were measured, corresponding to $RhAs_2$.

Assuming a parabolic growth rate (14), the activation energy, E_a, of the reaction can be calculated using the thickness of the reacted layer as a function of temperature. The Arrhenius plot of diffusivity (D= thickness ^{2}/time) versus temperature follows and exponential relation of

$$D = D_o \exp^{(-E_a/kT)}$$

where k= Boltzmann's constant (figure 9). The slope of this plot yields an activation energy of 1.35 $\pm$ .1 eV for the reaction. This is a similar value as previously reported of 1.65eV (13).

Discussion

The results obtained from planview electron diffraction display the changes in crystallographic orientation of the reacted layer with temperature. Texturing of the reacted phases reduces with temperature, implying an entropic effect of increasing the number of lowest energy configurations of the interface between the the reacted layer and the substrate at higher temperature. Grain size was uniform and increased with annealing temperature. The diffraction pattern at 700°C gives a clear idea of the final phases formed in the reaction being weakly textured $RhAs_2$ and oriented RhGa. The orientation of RhGa is also seen at 500° and speculated at 400° based on the intensity of the 0.301 and 0.215 nm reflections at 90°. The perferred orientation relationship is reported in results and figure 7. This orientation is different from CoGa and NiGa thin films which show $<001>_{MGa}$ // $<001>_{GaAs}$ (10). The mismatch between $<001>_{MGa}$ and $<001>_{GaAs}$ is greater for RhGa (6.5%) than for CoGa (1.8%) or NiGa (2.8%) leading to the observation that the unrotated orientation of Rh

with GaAs is not energetically favorable for RhGa.

It has been suggested in the past that untextured structure is not in contact with the substrate. This assumes that a preferred orientation will lower the interfacial surface energy. For $RhAs_2$, at temperatures above 500° only a weakly textured orientation was observed. This is probably due to the low symmetry of the monoclinic phase and the lack of a low energy arrangement of the interface. This argument supports the idea of a phase change from RhAs to RhAs2 around 400° on the basis of texturing of the polycrystalline reacted layer. In this experiment, the grain size of the reacted layer (54 nm at 700°) was larger than the thickness of the deposited metal so the phase separation is lateral to reduce interfacial surface area between RhGa and $RhAs_2$, attested to by the intimate contact between both reacted phases and the GaAs substrate.

In the early stage of the reaction, the reaction products are not conclusive. The interplanar spacings and the angles between planes of the same spacing of RhAs (orthorhombic) and $RhAs_2$(monoclinic) are too similar to be resolved. The presence of RhAs is supported at low temperatures by using arguments about texturing where RhAs is formed first since the higher symmetry structure can more effectively arrange its interface with the substrate to minimize the interfacial energy. The RhAs phase has been reported at 350° (12) and 450° (15) using x-ray diffraction and RBS, but since the spacings of the two RhAs phases are so similar, caution must be applied before distinguishing between reflections which are less than 1% different. Conclusive evidence of the presence of $RhAs_2$ at 400° was obtained from electron diffraction in this study using the (111) spacing of $RhAs_2$ which is significantly different (4%) than spacings of RhAs. 400° is when the barrier height drops (figure 1). This could indicate RhAs is an initial metastable phase and $RhAs_2$ forms at a slightly higher temperature. But the presence of RhAs is not certain; the reflections at 300° could be $RhAs_2$ where

no confirming $(11\overline{1})$ reflections near the [100]GaAs pole are found due to the orientation of the reacted phase with GaAs. In a systematic tilting experiment where the angular relationships between reflections were measured and compared with calculated angles for RhAs and $RhAs_2$ the presence of these two phases could be distinguished. The reaction of Rh and Ga may be similar to the Pt system where intermediate metal-rich phases form; the reflections for RhGa are very low intensity at 300° (2). This may be due to a preferential reaction between Rh and As or the formation of a yet undetected RhGa phase. Detection may be limited by thickness or swamped by the RhAs phase reflections.

Cross sectional TEM revealed a layered structure of Rh/RhGa/$RhAs_2$/GaAs, assuming the equilibrium $RhAs_2$ is present rather than RhAs. The images show voiding at the Rh/RhGa interface. This suggests Rh is a moving species and the voids are Kirkendall in nature. They are coalesced vacancies caused by net out-diffusion of Rh into the reacted layer. The separation of the As and Ga phases indicate Ga is also a moving species. The reaction process is diffusion-limited based the Arrhenius plot which assumes a parabolic rate of growth for the reacted layer. Figure 9 shows the plot yielding an activation energy of 1.35eV. This activation energy is similar to results using a more accurately determined diffusion coefficient where E_a was found to be 1.65eV (14). These values are comparable to those obtained for the formation of near noble metal silicides.

Lattice resolution imaging was used to determine the spatially resolved phase distribution. Lattice fringes of $RhAs_2$ were measured in contact with the GaAs substrate for columnar grains and spacings for RhGa were measured above these for equiaxed grains. These results of a layered structure of RhGa/$RhAs_2$/GaAs are in keeping with RBS data from similar samples (12), RBS also shows Ga in the As layer. The lattice fringe images were taken on the <110> GaAs pole indicating some orientation of the films with the substrate. Separa-

tion of the MGa and the MAs phases vertically with the MAs phase in contact with the GaAs has also been reported for Pt (2) and Ir (11). Other near noble metals separate laterally (Ni, Pd, Co) (9,10). Rh forms larger grains than Pt or Ir, which limits the extent of separation possible, resulting in an interpenetrated microstructure. The ratio of the separated RhGa to RhAs2 is ~1:4 which implies there is RhGa mixed with the RhAs2 phase if stoichiometry is assumed. The orientation relationship of the RhGa with GaAs is conserved in the thick (60nm) film suggesting contact between RhGa and GaAs (10) which is further argument for the mixing of the RhGa and the RhAs phases. An interesting feature to note is the columnar growth of the $RhAs_2$ grains, indicating a kinetically favored growth direction perpendicular to the substrate.

The leakage current measured for Rh/GaAs contact is a function of temperature where the endpoints have better electrical behavior than the leaky middle. This could be due to a phase change from metastable RhAs to RhAs2 as previously reported (12). Another interesting possibility is that the barrier height of the contact is a function of morphology of the interface between the reacted layer and GaAs. At 450° the interface is smooth, but at 400° there is roughness on the order of 10 nm, which is not noticeable at 350°. Roughness at the interface can cause high field regions which result in an effective lowering of the barrier height by tunneling electrons leaking through the barrier or chemical mixing at the metal/GaAs interface (16). Interface roughness has been related to low resistance current paths for ohmic contacts (17). The kinetics to grow smooth interfaces between reacted layers and GaAs may then be the critical consideration for making good contacts with reacted metal layers.

Conclusions

In this investigation the Rh/GaAs reaction was studied using the transmission electron microscope to look at the phases, position and morphology of the reacted Schottky contact. This information contributes some possible explaination for the unusual behavior of the Rh contact where the measured barrier height is a function of temperature (figure 1). Planview examination of thin (12 nm) films between 300 ° C and 700 ° show large changes in crystallographic orientation of the reacted layer with temperature. Though the initial phases could not be determined conclusively, the final phases are unambiguously $RhAs_2$ and RhGa. The RhAs-phase was difficult to to distinguish because of its low symmetry and high similarity to other product phases. The amount of texturing of the RhAs-phase went down with increasing temperature, showing strong texture at low temperature. This may be supporting evidence for a phase change at 400 ° or just an effect of entropy. The RhGa showed a well defined prefered orientation relationship of

$$\langle 011 \rangle \mathrm{RhGa} \; // \; \langle 022 \rangle \mathrm{GaAs}$$

$$\langle 011 \rangle \mathrm{RhGa} \; // \; \langle 0\bar{2}2 \rangle \mathrm{GaAs}$$

$$[0\bar{1}1]\mathrm{RhGa} \; // \; [100]\mathrm{GaAs}.$$

The presence of RhGa at the lowest temperature is questionable and may form an initial higher Rh content phase at low temperature, as does Pt (9).

Cross sections showed a layered structure of Rh/RhGa/$RhAs_2$. Voiding at the Rh/RhGa interface indicates Rh is the dominant diffusing species; E_a was calculated as 1.35 eV. An interpenetrated structure where RhGa is mixed with the $RhAs_2$ is observed. The $RhAs_2$ grains are columnar, indicating a kinetically favored growth direction. The interface roughness between the reacted layer and GaAs changed with annealing temperature. Roughness on the order of 10 nm is seen at 400 ° C but not found at 350 ° or 450 ° . This interfacial

morphology may contribute to the electrical behavior of the Rh contact.

Acknowledgements

Thanks to all who have taught me what I've learned here and Berkeley. Special thanks to Ron Gronsky, Byung Teak Lee and the rest of the Gronsky group, Jack Washburn, Tim Sands, Kin Man Yu, Dave, Lawrence, and my E45 students. I *think* its been worth it. This work is partially supported by the Director, Office of Basic Energy Research, Office of Energy Sciences, Materials Science Division of the U.S. Department of Energy.

References

[1] A.K. Sinha and J.M. Poate, Appl. Phys. Lett. **23**, 666 (1973).

[2] C. Fontaine, T. Okumura, and K.N. Tu, J. Appl. Phys. **54**, 1404 (1983).

[3] C.C. Chang, S.P. Murarka, V. Kumar, and G. Quintana, J. Appl. Phys. **46**, 4237 (1975).

[4] M. Ogawa, J. Appl. Phys. **51**, 406 (1980).

[5] T.S. Kuan, P.E. Batson, T.N. Jackson, H. Rupprecht, and E.L. Wilkie, J. Appl. Phys. **54**, 6052 (1983).

[6] Z. Liliental-Weber, R. Gronsky, J. Washburn, N. Newman, W.E. Spicer, E.R. Weber, J. Vac. Sci. Technol. B 4 **4**, 912 (1986).

[7] H.R. Grinolds, G.Y. Robinson, Solid State Electronics **23**, 973 (1980).

[8] T. Sands, V.G. Keramidas, R. Gronsky, and J. Washburn, Thin Solid Films, **136**, 105 (1986).

[9] T. Sands, V.G. Keramidas, A.J. Yu, K.M. Yu, R. Gronsky, and J. Washburn, J. Mater. Res., submitted.

[10] T. Sands, V.G. Keramidas, K.M. Yu, J. Washburn and K. Krishnan, J. Mater. Res., submitted.

[11] K.M. Yu, T. Sands, J.M. Jaklevic, and E.E. Haller, J. Appl. Phys., in press.

[12] K.M. Yu, S.K. Cheung, T. Sands, J.M. Jaklevic, and E.E. Haller, J. Appl. Phys. **61**, 1099 (1987).

[13] K.M. Yu, J.M. Jaklevic, E.E. Haller, Mater. Res. Soc. Symp. Proc. **69**, 281 (1986); Nucl. Istrum. Methods B10/11, 606 (1985)

[14] K.M. Yu, Ph.D. Thesis, UC Berekely, 1987.

[15] C.J. Todd, J.D. Speight, G.W.B. Ashwell and R. Heckingbottom, ECS Extended Abstracts #114, Spring Meeting, Toronto, 75:1, p274 (1975).

[16] N. Braslau, J. Vac. Sci. and Technol., **19**(3), 803 (1981).

[17] W. Walukiewicz, J. Vac. Sci and Technol., submitted 2/87.

Figure Captions

Figure 1. a) Ideality factor n and Schottky barrier height ϕ_B measured by IV techniques for Rh/n-GaAs diodes as deposited and annealed for 20 minutes. (b) The leakage current density at -0.4V bias for diodes annealed at different temperatures for 20 min.

Figure 2. a) Transmission electron diffraction of 12 nm Rh on GaAs after annealing 20 min. showing textured reaction products and unreacted Rh rings. B=[100]GaAs. (b) TEM image of same specimen shoeing small grain size ~ 6.5 nm. (c) Schematic of diffraction pattern is shown for the reacted layer with d-spacings of$RhAs_2$

Figure 3. Rh/GaAs specimen annealed at 400°C for 20 min. (a) DP shows a ring-like pattern at 0.215 nm. (b) Average grain size is 12 nm. (c) Schematic of reaction products and $RhAs_2$ spacings.

Figure 4. 12 nm Rh on GaAs annealed at 500° for 20 min. (a) B=[100]GaAs, DP has less texture, and shows 0.393 nm and 0.517 nm spacings from $RhAs_2$. (b) Average grain size is 29 nm. (c) Schematic of DP.

Figure 5. 700° 20 min. 12 nm Rh/GaAs. (a) B=[100]GaAs and $[0\bar{1}1]$RhGa, arrows indicate the rectangular RhGa pattern, $RhAs_2$ produces weakly textured rings. (b) Large grains ~ 54 nm, some show twinning. (c) Schematic of $RhAs_2$ reflections.

Figure 6. Shows the orientations relationship between RhGa and GaAs.

Figure 7. a) Cross sectional micrograph of 60 nm thick Rh on GaAs showing a layered structure after annealing at 350° for 20 min. (b) B=[110] (c) Schematic of phases present.

Figure 8. TEM image of Rh/GaAs annealed at 400° for 90 min. (a) Shows a layered structure and arrows point out columnar grains. (b) A thicker region of the specimen shows the interface morphology. Arrows point out protrusions. (c) Schematic.

Figure 9. a) TEM micrograph of RhGaAs after annealing at 450° for 20 min. Grains are larger and the interface smooth. (b) B=[110]GaAs (c) Schematic

Figure 10. An Arrhenius plot of diffusivities deduced from reaction layer thickness assuming a parabolic growth rate, versus annealing temperatures

Table 1. 300° C 20 minute anneal

spacings	$RhAs_2$ monoclinic		RhAs orthorhombic		RhGa fcc		Rh fcc	
nm	nm	( )	nm	{ }	nm	{ }	nm	{ }
0.617	0.608	010 [a]	0.600	001 [b]				
0.554	0.558	001 [a]	0.565	100 [b]				
	0.550	100 [a]						
	0.511	$10\bar{1}$ [a]						
	0.411	011 [a]	0.411	110				
	0.393	$11\bar{1}$, $1\bar{1}\bar{1}$	0.307	011				
0.303	0.304	020	0.300	002	0.301	100		
0.279	0.279	002	0.283	200				
	0.275	200						
0.274	0.273	$1\bar{1}\bar{2}$, $11\bar{2}$						
	0.270	$21\bar{1}$, $2\bar{1}\bar{1}$ [a]	0.270	111				
	0.267	021, $02\bar{1}$ [a]						
0.266	0.266	120	0.265	102				
	0.261	$1\bar{2}\bar{1}$						
	0.254	012, $01\bar{2}$						
	0.251	210, $2\bar{1}0$						
	0.237	$2\bar{1}\bar{2}$	0.222	210			0.220	111
0.212	0.215	102, $1\bar{2}\bar{2}$	0.213	112	0.213	110		

[a] calculated $RhAs_2$ spacings not verified with ASTM card 14-414, $RhAs_2$
[b] calculated RhAs spacings not verified with ASTM card 7-384, MnP

Table 2. 400 ° C 20 minute anneal

spacings nm	$RhAs_2$ monoclinic nm	( )	RhAs orthorhombic nm	{ }	RhGa fcc nm	{ }	Rh fcc nm	{ }
0.623	0.608	010 [a]	0.600	001 [b]				
0.567	0.558	001 [a]	0.565	100 [b]				
	0.550	100 [a]						
	0.511	$10\bar{1}$ [a]						
0.417	0.411	011 [a]	0.411	110				
0.394	0.393	$11\bar{1}$, $1\bar{1}\bar{1}$	0.307	011				
0.305	0.304	020	0.300	002	0.301	100		
	0.279	002	0.283	200				
	0.275	200						
0.272	0.273	$1\bar{1}\bar{2}$, $11\bar{2}$						
	0.270	$21\bar{1}$, $2\bar{1}\bar{1}$ [a]	0.270	111				
	0.267	021, $02\bar{1}$ [a]						
	0.266	120	0.265	102				
	0.261	$1\bar{2}\bar{1}$						
0.254	0.254	012, $01\bar{2}$						
	0.251	210, $2\bar{1}0$						
	0.237	$2\bar{1}\bar{2}$	0.222	210			0.220	111
0.213	0.215	102, $1\bar{2}\bar{2}$	0.213	112	0.213	110		

[a] calculated $RhAs_2$ spacings not verified with ASTM card 14-414, $RhAs_2$
[b] calculated RhAs spacings not verified with ASTM card 7-384, MnP

Table 3. 500 ° C 20 minute anneal

spacings	$RhAs_2$ monoclinic		RhAs orthorhombic		RhGa fcc		Rh fcc	
nm	nm	( )	nm	{ }	nm	{ }	nm	{ }
	0.608	010 [a]	0.600	001 [b]				
	0.558	001 [a]	0.565	100 [b]				
	0.550	100 [a]						
0.517	0.511	$10\bar{1}$ [a]						
	0.411	011 [a]	0.411	110				
0.393	0.393	$11\bar{1}$, $1\bar{1}\bar{1}$	0.307	011				
0.300*	0.304	020	0.300	002	0.301	100		
0.279	0.279	002	0.283	200				
	0.275	200						
	0.273	$1\bar{1}\bar{2}$, $11\bar{2}$						
	0.270	$21\bar{1}$, $2\bar{1}\bar{1}$ [a]	0.270	111				
	0.267	021, $02\bar{1}$ [a]						
0.265	0.266	120	0.265	102				
	0.261	$1\bar{2}\bar{1}$						
0.254	0.254	012, $01\bar{2}$						
	0.251	210, $2\bar{1}0$						
	0.237	$2\bar{1}\bar{2}$	0.222	210			0.220	111
0.215*	0.215	102, $1\bar{2}\bar{2}$	0.213	112	0.213	110		

[a] calculated $RhAs_2$ spacings not verified with ASTM card 14-414, $RhAs_2$
[b] calculated RhAs spacings not verified with ASTM card 7-384, MnP
* strong 90 ° axial intensities

Table 4. 700 ° C 20 minute anneal

spacings	$RhAs_2$ monoclinic		RhAs orthorhombic		RhGa fcc		Rh fcc	
nm	nm	( )	nm	{ }	nm	{ }	nm	{ }
	0.608	010 [a]	0.600	001 [b]				
	0.558	001 [a]	0.565	100 [b]				
	0.550	100 [a]						
0.514	0.511	$10\bar{1}$ [a]						
	0.411	011 [a]	0.411	110				
0.393	0.393	$11\bar{1}$, $1\bar{1}\bar{1}$	0.307	011				
0.301*	0.304	020	0.300	002	0.301	100		
0.278+	0.279	002	0.283	200				
	0.275	200						
	0.273	$1\bar{1}\bar{2}$, $11\bar{2}$						
	0.270	$21\bar{1}$, $2\bar{1}\bar{1}$ [a]	0.270	111				
	0.267	021, $02\bar{1}$ [a]						
0.265+	0.266	120	0.265	102				
	0.261	$1\bar{2}\bar{1}$						
0.255+	0.254	012, $01\bar{2}$						
	0.251	210, $2\bar{1}0$						
	0.237	$2\bar{1}\bar{2}$	0.222	210			0.220	111
0.215*	0.215	102, $1\bar{2}\bar{2}$	0.213	112	0.213	110		

[a] calculated $RhAs_2$ spacings not verified with ASTM card 14-414, $RhAs_2$
[b] calculated RhAs spacings not verified with ASTM card 7-384, MnP
* strong 90 ° axial intensities
+ many reflections of similar spacings present

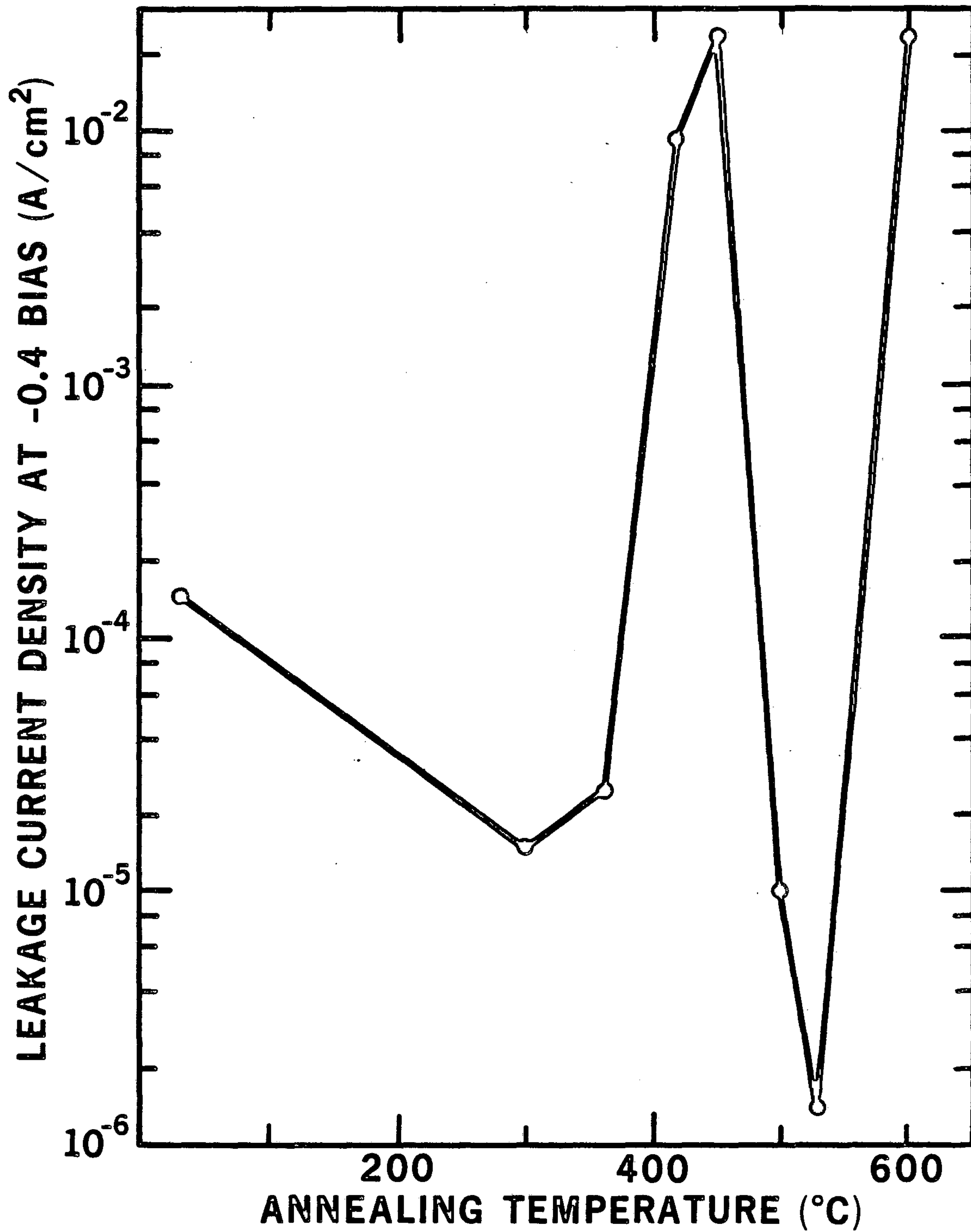

XBL 865-1928

Fig 1

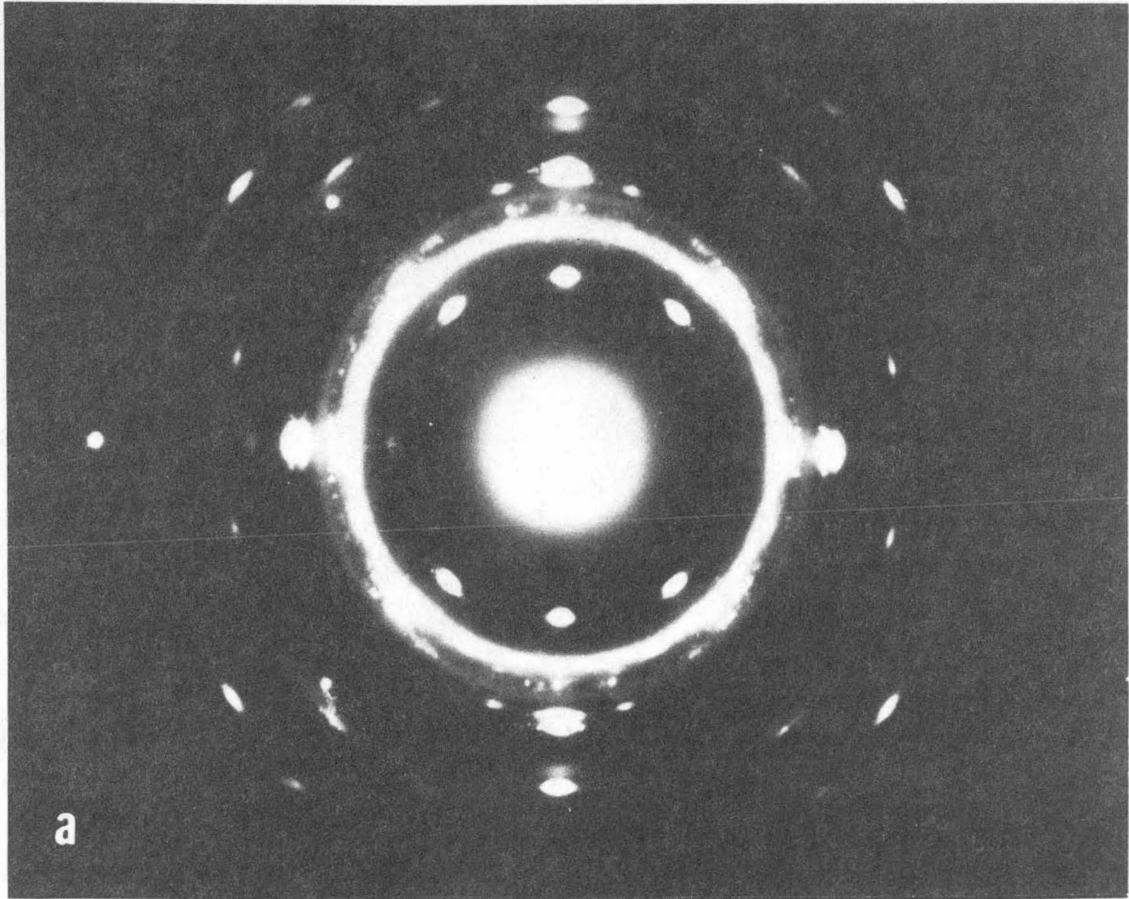

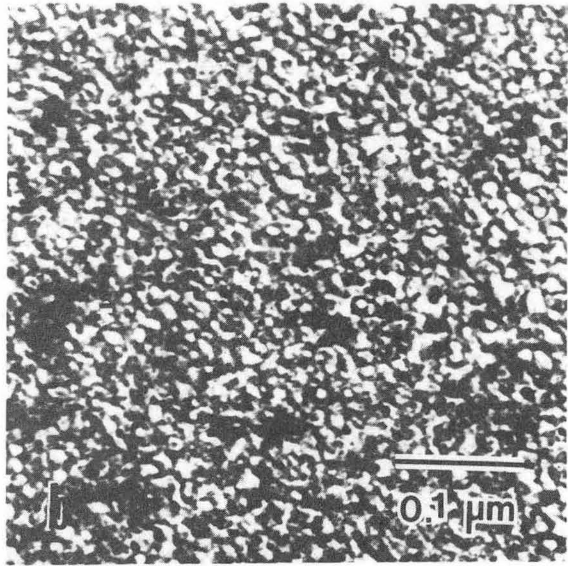

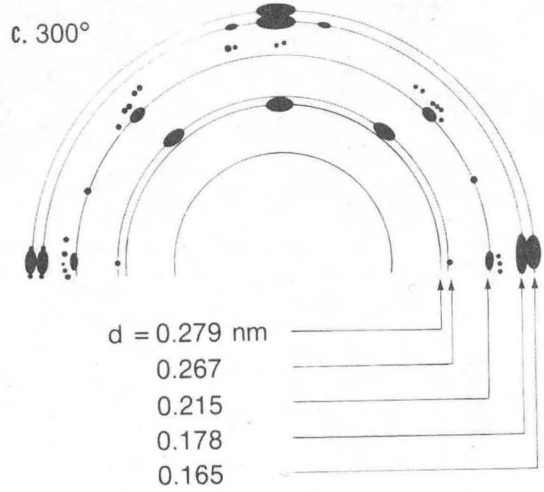

Fig 2

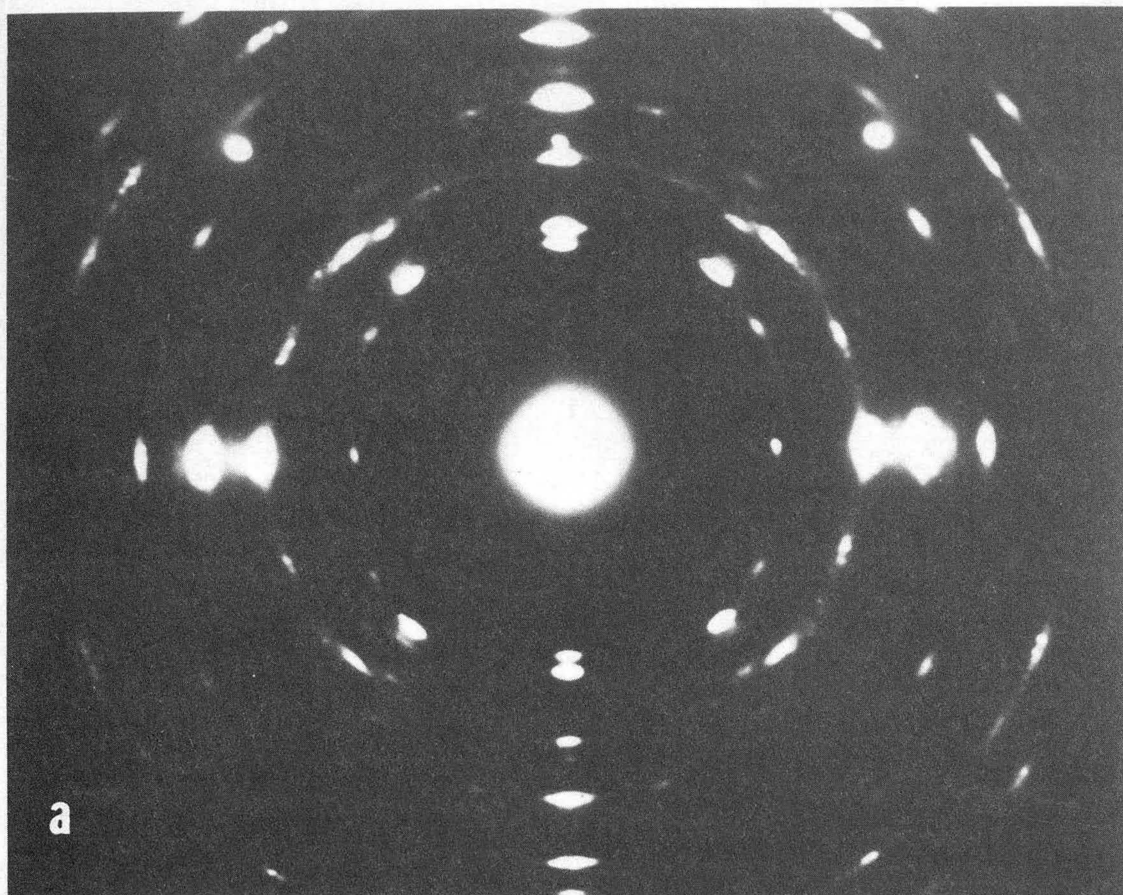

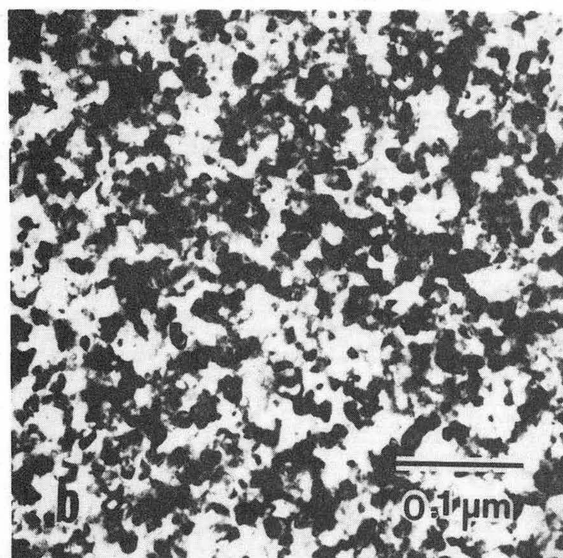

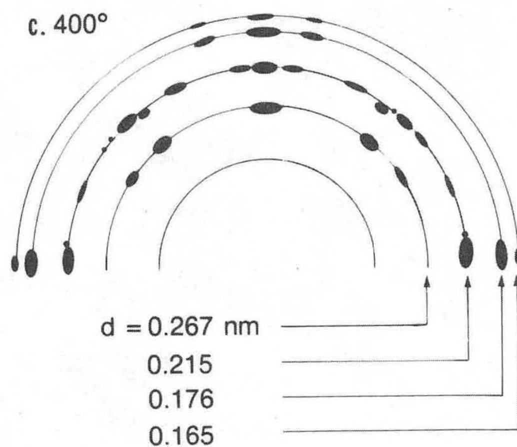

XBB 875-3969

Fig 3

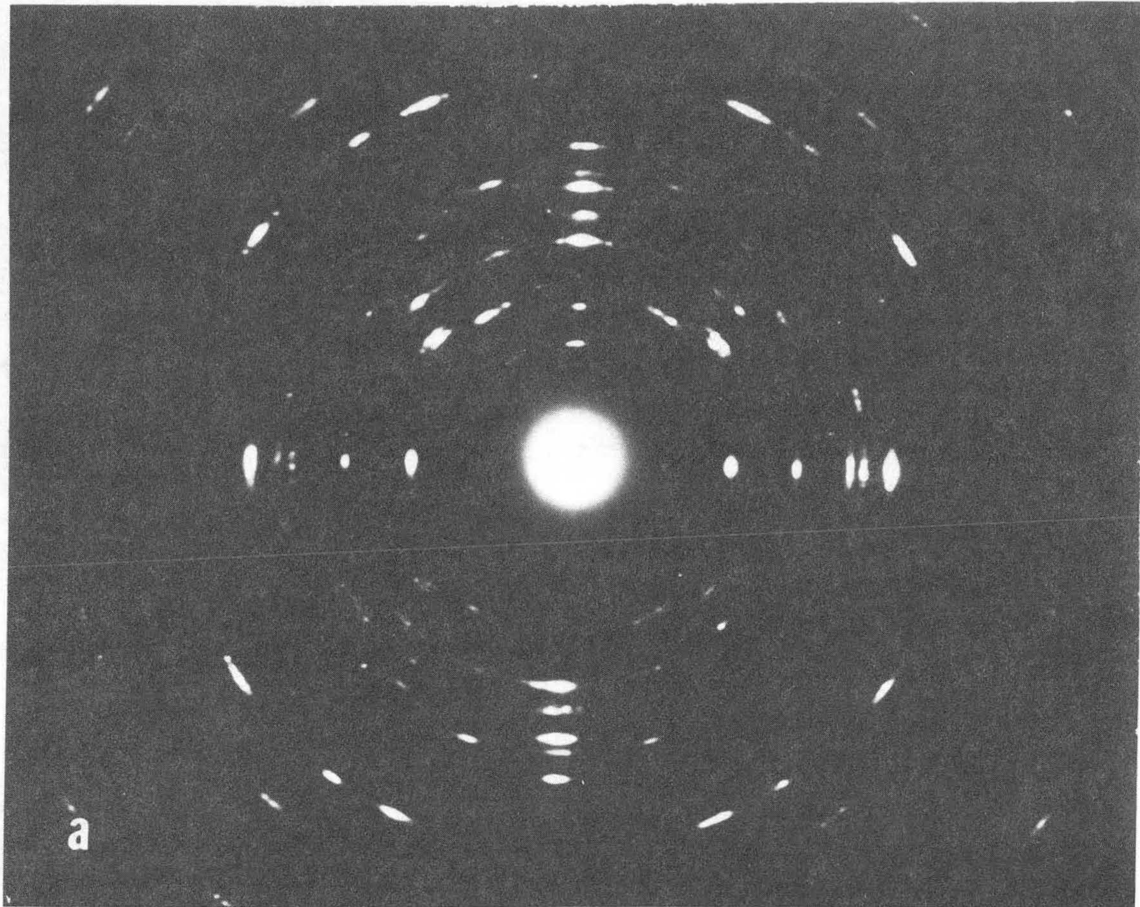

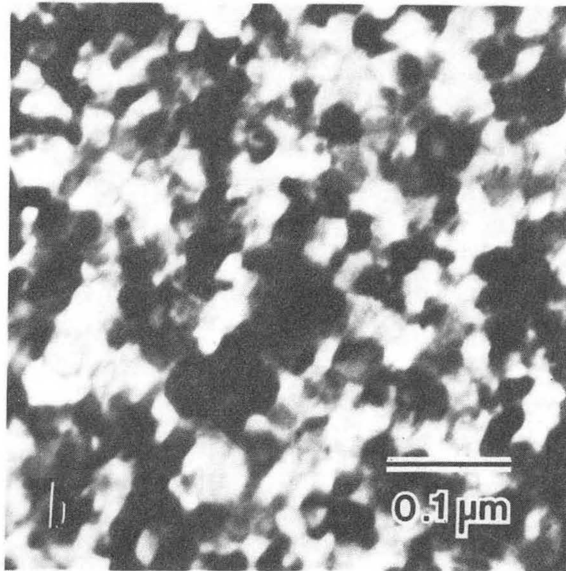

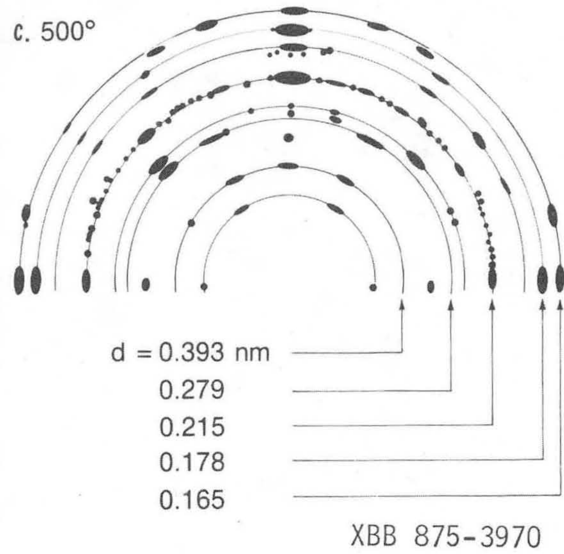

Fig 4

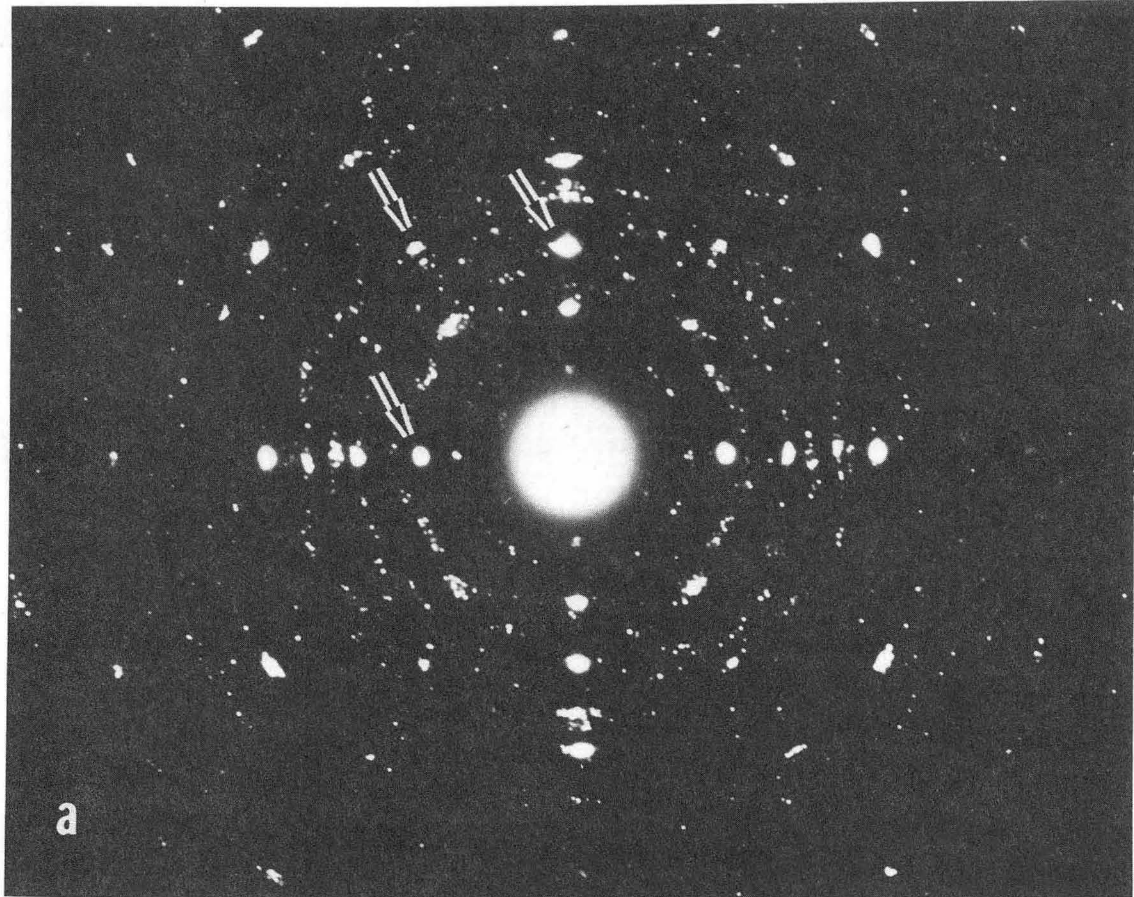

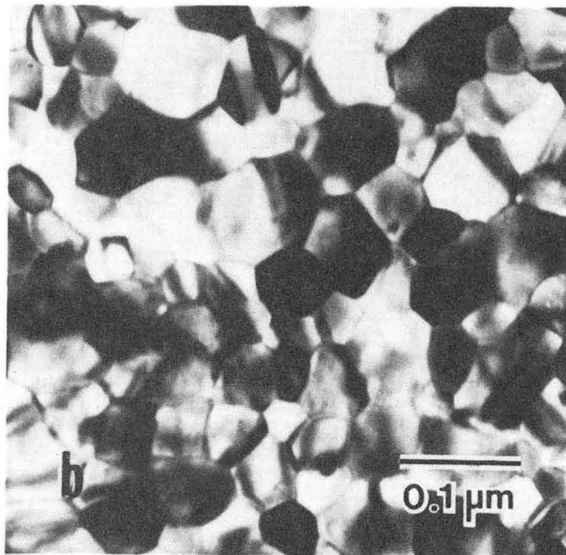

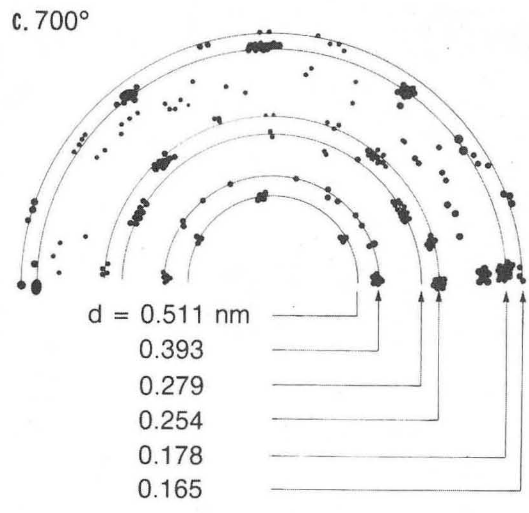

Fig 5

Orientation Relationships between RhGa and GaAs

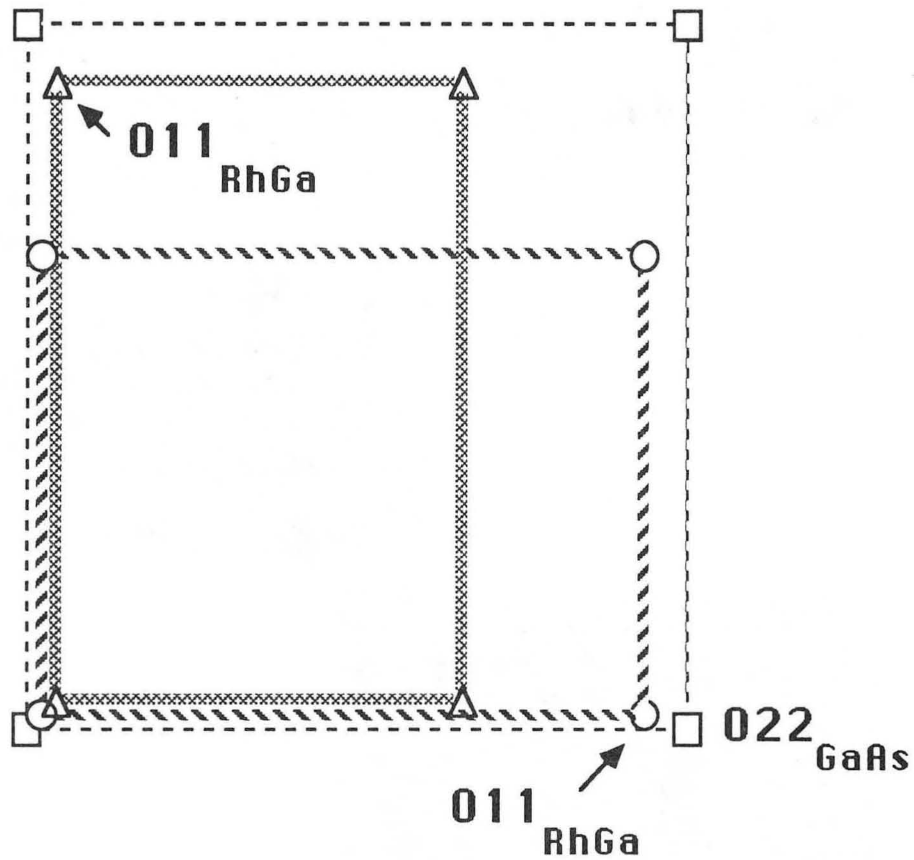

$\langle 011 \rangle_{RhGa} \; // \; \langle 022 \rangle_{GaAs}$

$\langle 011 \rangle_{RhGa} \; // \; \langle 0\bar{2}2 \rangle_{GaAs}$

$[0\bar{1}1]_{RhGa} \; // \; [100]_{GaAs}$

Fig 6

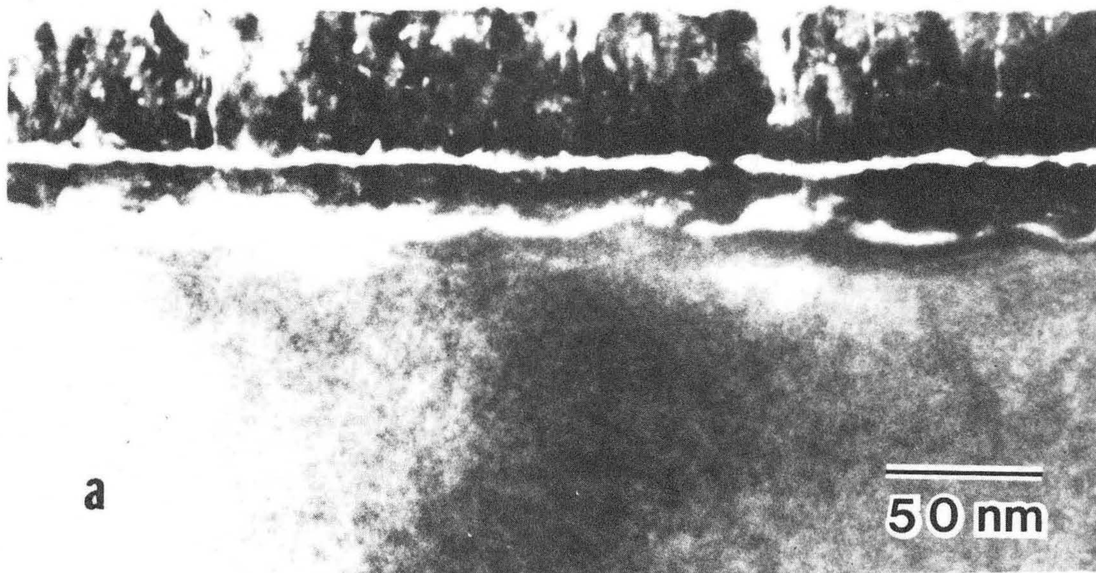

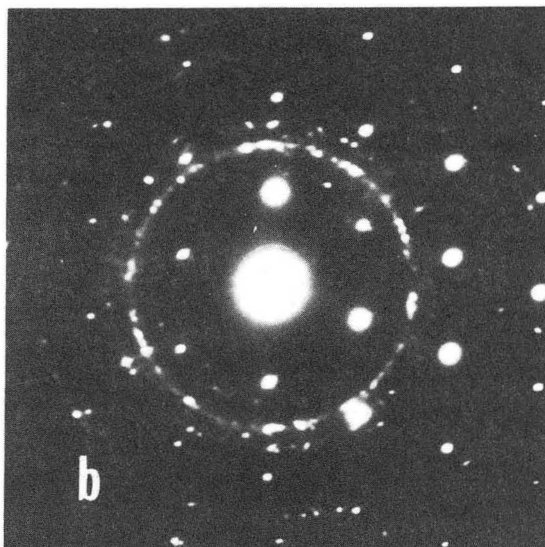

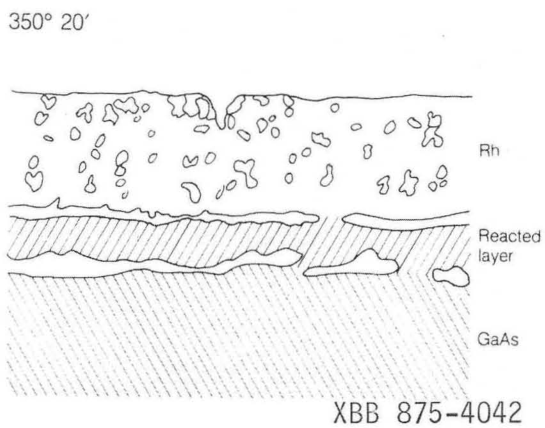

XBB 875-4042

Fig 7

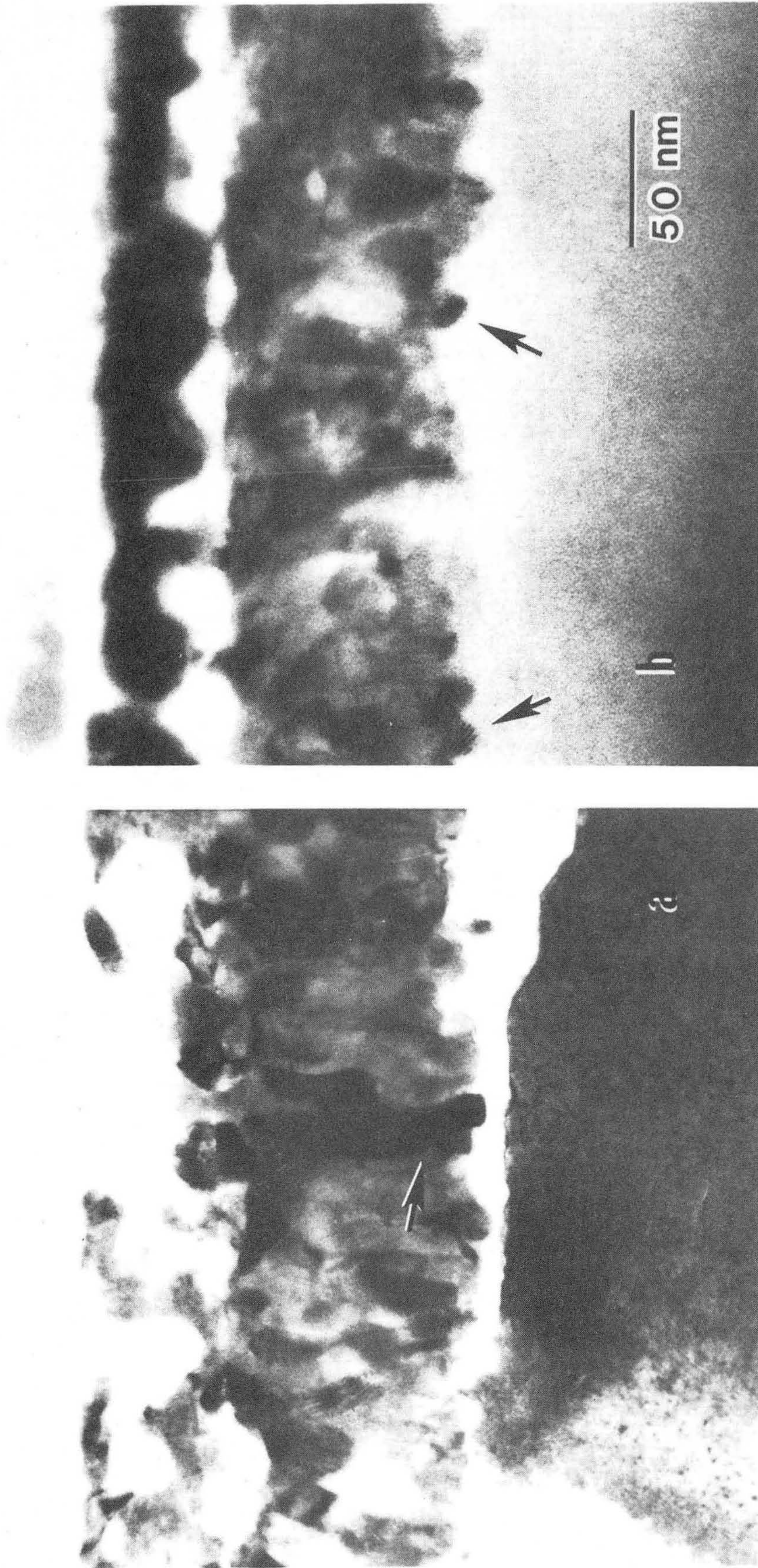

Fig 8

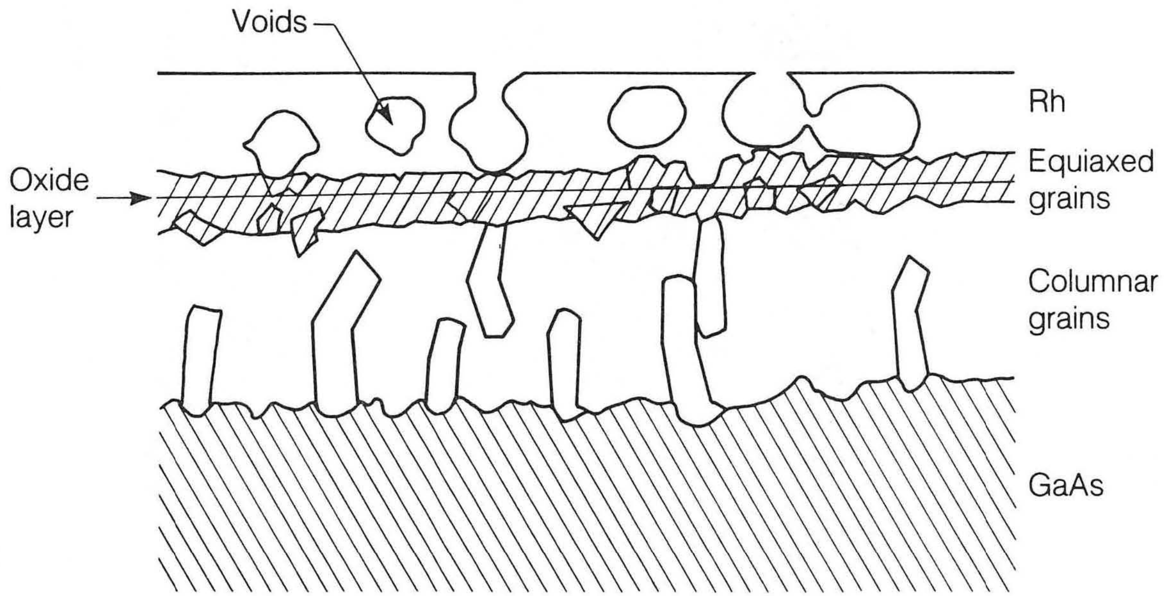

Fig 8c

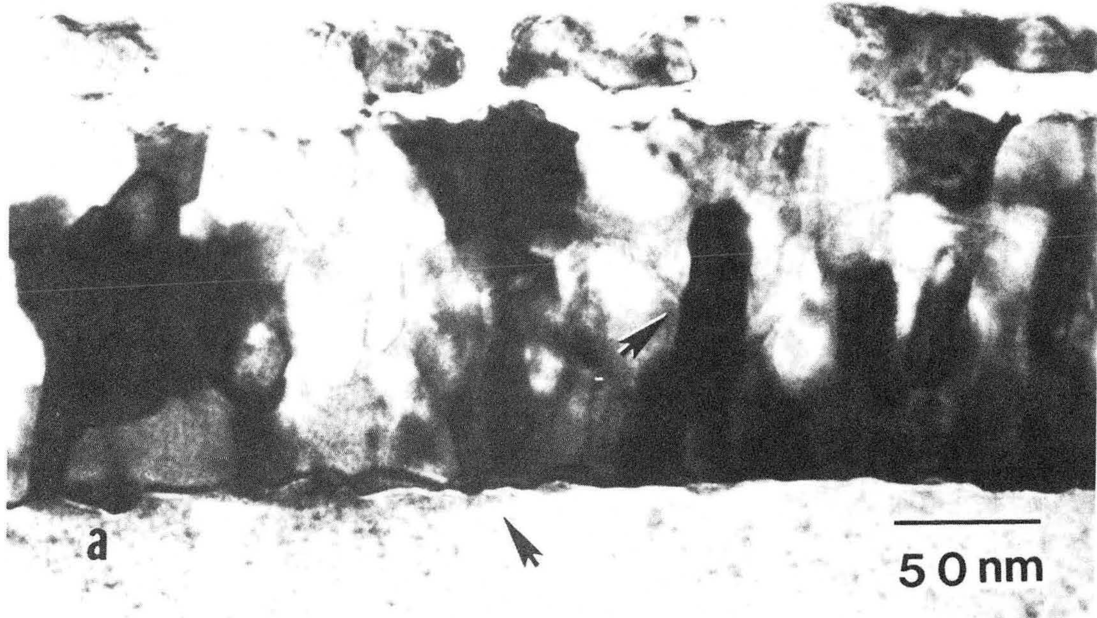

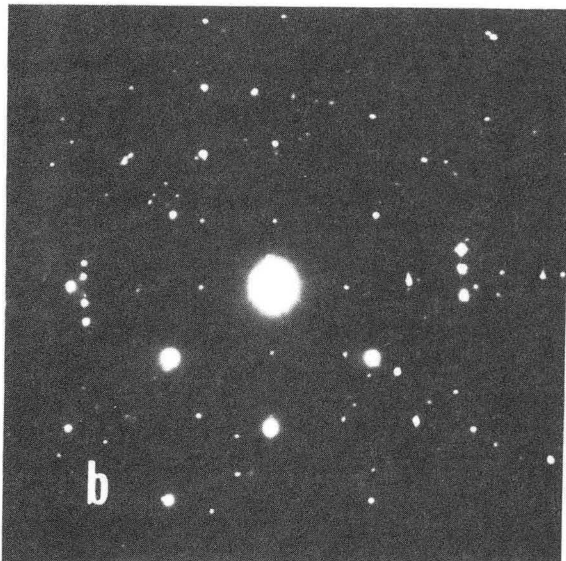

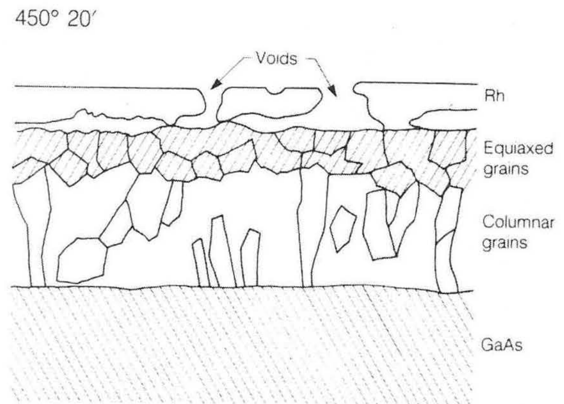

XBB 875-4043

Fig 9

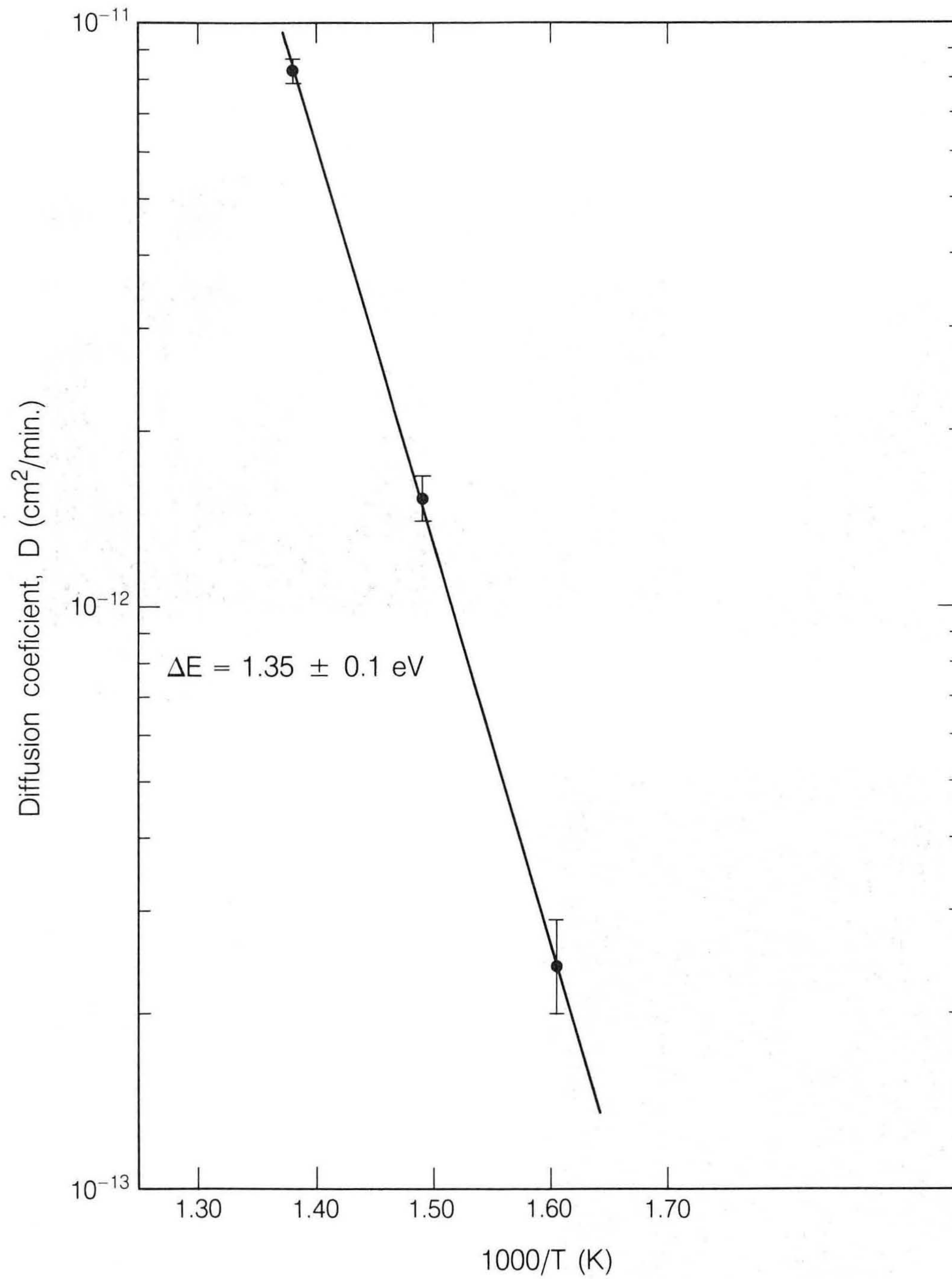

XBL 875-9041

Fig 10

LAWRENCE BERKELEY LABORATORY
TECHNICAL INFORMATION DEPARTMENT
UNIVERSITY OF CALIFORNIA
BERKELEY, CALIFORNIA 94720